UPPSALA
UNIVERSITET

The pH dependence of peptide release from the ribosome

Gabriele Indrisiunaite

Degree project in biology, Master of science (2 years), 2012
Examensarbete i biologi 45 hp till masterexamen, 2012
Biology Education Centre and Department of Cell and Molecular Biology, Uppsala University
Supervisor: Michael Pavlov
External opponent: Johan Sund

Table of contents

Summary

We have employed two different fast kinetic methods to study the pH dependence of the rate of peptide release reaction (termination) in protein synthesis. To this end we have used a classic quench flow technique and a newly developed stop flow approach that relies on the use of fluorescently labeled peptides. We demonstrate that the pH dependence of the peptide release reaction is compatible with the reaction scheme in which a hydroxide ion, not a water molecule, participates in the release factor catalyzed hydrolysis of ester bond between peptide and tRNA in the P-site of the ribosome. Moreover, our data indicates the presence of a fast conformational step on the reaction pathway that precedes the chemical reaction of the ester bond hydrolysis. We have also measured the kinetics of peptide release from stalled ribosome complexes containing UGG codon in the A site. The measured values confirm the previous conclusions about an exceptionally high fidelity of the termination reaction.

Abbreviations

Cm	Fluorescent label, methoxy-coumarin
DTE	1,4-dithioerythritol
FA	Formic acid
HEPES	4-(2-hydroxyethyl)-1-piperazineethanesulfonic acid
HPLC	High pressure liquid chromatography
MFF	fMet-Phe-Phe tripeptide
Mq	Fluorescent label, aminomethyl-coumarin
mRF1/mRF2	Methylated release factor 1/release factor 2
PEP	phosphoenolpyruvate
QF	Quench flow
RC	Release complexes
RF	Release factor
SF	Stopped flow
uRF1	Unmethylated release factor 1
PTC	Peptidyl transfer centre
MM	Materials and methods

1. Introduction

1.1. Class I release factors

Translation termination is a process when finished peptide is released from the ribosome (reviewed in Kisselev et al., 2003; Korostelev, 2011; Youngman et al., 2008). It occurs when a translating ribosome encounters one of the in-frame stop codons (UAA, UAG or UGA) on mRNA. These codons do not have corresponding tRNAs, but are instead recognized by class I release factors (RF). These factors bind to the A site of the ribosome, recognise the stop codon and trigger the hydrolysis of the ester bond between the finished peptide and the tRNA in the P-site of the ribosome. This severs the main link holding the peptide on the ribosome and leads to its release into solution.

Bacteria have two RFs with overlapping codon specificity: RF1 recognises UAA and UAG while RF2 recognizes UAA and UGA (Ito et al., 2000). It has been initially suggested that the bacterial release factors recognise stop codons using tripeptide anticodon motifs: P(A/V)T in RF1 and SPF in RF2 (Ito et al., 2000). However, both structural studies (Korostelev et al., 2010; Laurberg et al., 2008) and molecular dynamics simulations (Sund et al., 2010) indicate that the actual recognition is more complex and involves a number of other amino acids (reviewed in Klaholz, 2011; Loh and Song, 2010). The recognition of a stop codon is believed to induce a conformational change in the factor that may switch on its catalytic activity (Korostelev, 2011). Bacterial RF1 and RF2 have a similar structure consisting of 4 domains (Fig. 1). The peptide

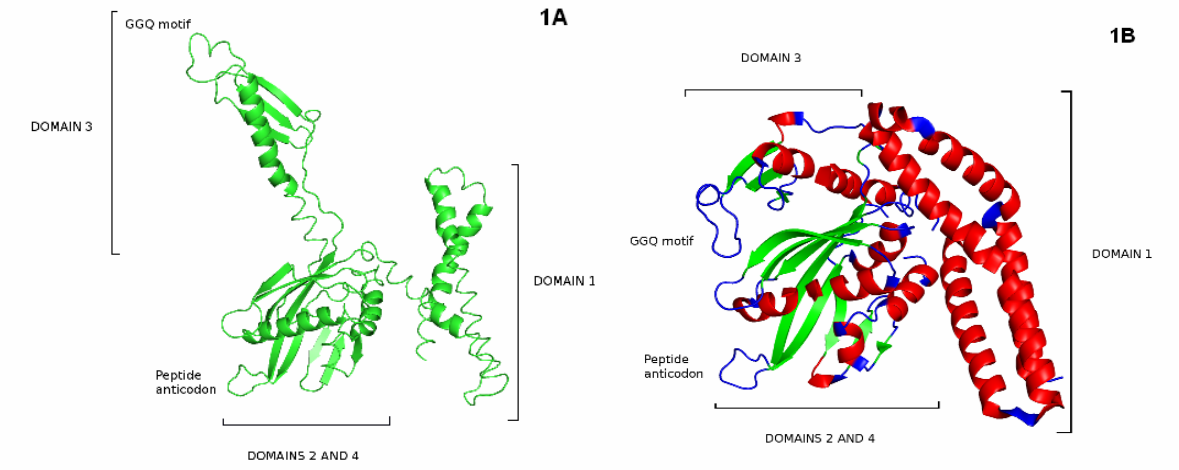

Figure 1. Crystal structures of prokaryotic class I release factors. 1A. *Thermus thermophilus* RF2 in an open conformation (PDB entry 2X9T). 1B. *Escherichia coli* RF2 in a closed conformation (PDB entry 1GQE).

anticodon is placed in domain 2 that is packed against domain 4 to form a rigid central core of the protein. Domain 3 contains a conserved glycine-glycine-glutamine (GGQ) motif which is placed in an extended loop that reaches into the peptidyl transfer centre (PTC) of the ribosome. N-terminal domain 1 is not essential for peptide release, but it interacts with class II release factor RF3 to promote RF dissociation from the ribosome after termination (Brunelle et al., 2008; Klaholz, 2011; Shin et al., 2004). The crystal structures of RFs in free form and on the ribosome are different. On the ribosome the factors have an open conformation with about 75 Å distance between the peptide anticodon and the GGQ motif (Jin et al., 2010; Klaholz et al., 2003; Korostelev et al., 2008; Laurberg et al., 2008) while the crystallized free factors have a closed conformation in which these regions are only about 25 Å apart (Shin et al., 2004; Vestergaard et al., 2001). It could mean that the RFs have to undergo a large structural change upon binding to the ribosome to achieve their active conformations. However, low resolution models obtained by small-angle X-ray scattering indicate that the solution conformation might also be an open one (Vestergaard et al., 2005). The puzzle if the closed conformation is functionally important or if it is a crystal artefact remains unresolved so far. Nevertheless, the very existence of the closed and open conformations seen by X-ray crystallography demonstrates the conformational flexibility of the RFs. It is possible therefore that some intermediate, half opened conformation of free RF might exist in solution.

1.2. The importance of GGQ motif

An important feature of RFs is a conserved glycine-glycine-glutamine (GGQ) motif that interacts with the peptidyl transferase centre (PTC) on the large ribosome subunit (Jin et al., 2010; Song et al., 2000). The universal presence of this motif in all class I release factors that seem to have evolved independently in different kingdoms of life gave the first idea of its importance for the peptide release reaction (Frolova et al., 1999; Kisselev et al., 2003). Further studies have shown that mutations of any of the three amino acids in this motive are lethal in vivo (Mora et al., 2003). Substitutions of any of the glycines almost completely abolish the release activity also in vitro (Mora et al., 2003; Shaw and Green, 2007; Zavialov et al., 2002). Such intolerance to Gly substitutions could be explained by the unique conformational flexibility of the glycine backbone, which may adopt conformations not possible for other amino acids to properly position the catalytic glutamine residue in the PTC of the ribosome (Song et al., 2000). This role of Gly residues was confirmed by computer simulations (Trobro and Aqvist, 2007) and crystal structures of complexes of release factors with ribosomes (Jin et al., 2010; Korostelev et al., 2008).

Song and co-workers have proposed that the glutamine residue (Q) plays an essential role in catalysis by coordinating the water molecule that performs a nucleophilic attack on the ester bond between the nascent peptide and P-site tRNA (Song et al., 2000). This direct role of Gln was questioned by the studies where substitutions of Gln with other amino acids had varying and in some cases rather small effect on the termination rates in vitro (Shaw and Green, 2007). The question about the effect of these Q-substitution is still open since the GGA mutation was reported to result in a 100-fold reduction in the catalytic rate k_{cat} of RF2 in one study (Zavialov et al., 2002) but only in a 4-fold reduction in the other (Shaw and Green, 2007). The partial activity of the GGA mutant could be explained by the small size of Ala side chain that allows an extra water molecule to occupy the space normally taken by the carbonyl oxygen of glutamine and provide hydrogen bonding for the water molecule participating in hydrolysis (Trobro and Aqvist, 2007). The mutations of Gln to asparagine (Asn) or aspartic acid (Asp) result in a large 7500-fold and 9500-fold decrease in k_{cat} of termination (Shaw and Green, 2007). Asparagine and aspartic acid are similar in structure to glutamine, but one carbon atom shorter. It is possible, that they can also coordinate the nucleophilic water molecule, but may place it too far away from the labile ester bond to participate effectively in catalysis (Shaw and Green, 2007). In addition to coordinating the nucleophilic water the glutamine residue also excludes larger nucleophiles such as hydroxyl-amine and probably larger alkyl-amines from the reaction site (Shaw and Green, 2007). Mutations to amino acids with smaller side chains reduced the specificity for water and increased the rate of aminolysis (Shaw and Green, 2007). It was also reported that the glutamine residue in GGQ motif undergoes a post-translational modification to N^5–methyl glutamine (Dincbas-Renqvist et al., 2000). This modification moderately increases the rate of termination by RF2 (Dincbas-Renqvist et al., 2000)

1.3. The reaction mechanism of peptide release

The peptidyl transferase centre (PTC) of the large ribosomal subunit catalyses two critical reactions of protein synthesis: the peptidyl transfer reaction and the peptide release. In both cases the chemical reaction is an attack of a nucleophile on the carbonyl carbon participating in the ester bond between the synthesized peptide and P-site tRNA (Shaw and Green, 2007). In the peptidyl transfer reaction the nucleophile is the amino group of the amino acid on the A-site tRNA. In peptide release, class I release factors coordinate and activate a water molecule that is the nucleophile in this reaction (Shaw and Green, 2007; Song et al., 2000). Peptide release is more chemically challenging, because water oxygen is a much weaker nucleophile than a primary amine of amino acid. The scheme of the peptide release suggested in Jin et al. (2010) is outlined in Fig. 2. Computational analysis suggests a proton shuttle mechanism for the reaction of ester

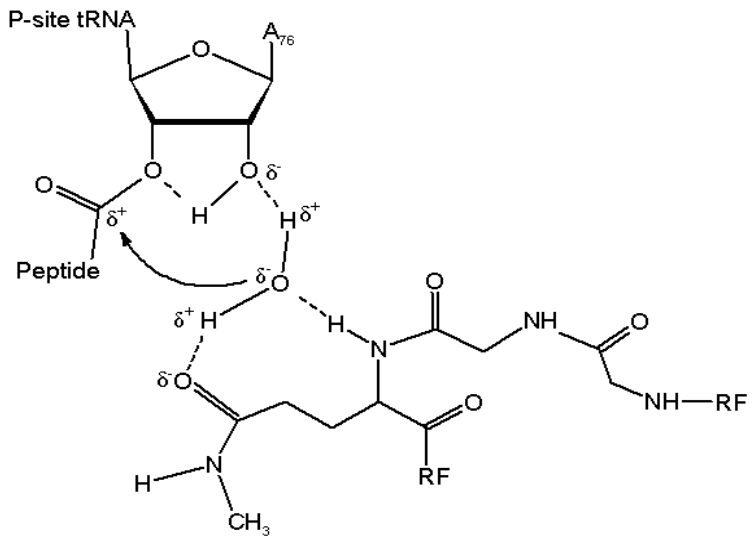

Figure 2. A reaction mechanism of peptide release suggested by Jin et al. (2010). The water oxygen performs a nucleophilic attack on the carbonyl carbon of the ester linkage between the P-site tRNA and the synthesized peptide. The catalytic water molecule is coordinated by the 2'-OH of the A76 of the P-site tRNA together with the side-chain carbonyl group and backbone amide of the glutamine residue belonging to the GGQ motif.

bond hydrolysis on the ribosome. In this mechanism a proton is transferred from the nucleophilic water to the 2'-OH and then to the 3'-O group of the A76 ribose of peptidyl-tRNA in the P-site. A protonated 3'-OH hydroxyl of A76 is a leaving group in this reaction (Trobro and Aqvist, 2009). In line with this proposed mechanism, substitutions at the A76 2'-OH position strongly inhibit peptide release by RF1 (Brunelle et al., 2008). It was also suggested by computational analysis that the amide oxygen of the glutamine of the GGQ motif forms a hydrogen bond with the nucleophilic water molecule and orients it for catalysis (Trobro and Aqvist, 2009). The backbone amide (NH) of the GGQ glutamine donates another hydrogen bond that positions the water nucleophile (see Fig. 2) and this interaction was proposed to be the major catalytic contribution of the release factor (Korostelev, 2011).

Despite of much modelling efforts, structural studies and a host of biochemical experimental data which were briefly outline above, the mechanism of the peptide release reaction is not completely understood. One of the riddles here is a strong pH dependence of the release reaction (Kuhlenkoetter et al., 2011). The rate of the release of the peptide mimic formylated methionine (fMet) from fMet-tRNA in the P-site of the ribosome increases linearly with the concentration of hydroxide ions in the reaction buffer. These pH titration results were interpreted as a titration of a group with a pKa more than 9 or as a participation of hydroxide ion (OH^-) in the reaction mechanism (Kuhlenkoetter et al., 2011). One potential caveat in the experimental setup in this study is the use of fMet-tRNA as a model of peptidyl-tRNA. It is

known that the rate of peptide release depends on the nature (Bjornsson et al., 1996) and length of the peptide attached to peptidyl-tRNA. The rate of release increases substantially when fMet is replaced by longer peptides fMet-Ile or fMet-Phe-Trp-Ile (Dincbas-Renqvist et al., 2000). It means that the linear dependence of the release rate on the concentration of hydroxide ion observed by Kuhlenkoetter et al. (2011) may be due to an artificially slow rate of the RF-catalyzed hydrolysis reaction with fMet peptide mimic. We therefore used a tri-peptidyl-tRNA carrying an MFF tripeptide that we show here can be released more then 10-fold faster than the fMet peptide mimic. We demonstrate that the pH dependence of the release rate is consistent with the participation of hydroxide ion in the reaction mechanism. The pH dependence of the release rate also exhibits saturation that may be interpreted as the presence of a rate limiting conformation step on the reaction pathway leading to the ester bond hydrolysis.

1.4. Aims

The pH dependency of peptide release by class I release factors was previously reported with fMet as peptide mimic (Kuhlenkoetter et al., 2011). The aim of this project was to look into the pH dependence of the rate of peptide release using tripeptidyl-tRNA and to compare the results obtained by two different fast kinetics methods: a classic quench flow approach and a newly developed stopped flow technique.

2. Results

2.1. Preparation and analysis of the release complexes

Studying of how a reaction rate changes with pH can provide useful information about catalytic groups participating in this reaction. We have investigated the effect of pH on the catalytic rate (k_{cat}) of peptide release by methylated RF1 and RF2 (wild type) and by RF1 lacking this modification. The time course of peptide release was monitored by two different fast kinetics methods: quench flow and stopped flow. In both cases purified RFs reacted with release complexes (RC) containing ribosomes stalled on a UAA stop codon in the A site and peptidyl-tRNA with labelled fMFF tripeptide in the P site (Fig. 3). In quench flow experiments the label was ^{3H}Met and the amount of released peptide was determined by scintillation counting as described in Materials and Methods (MM). In stopped flow experiments we used two different

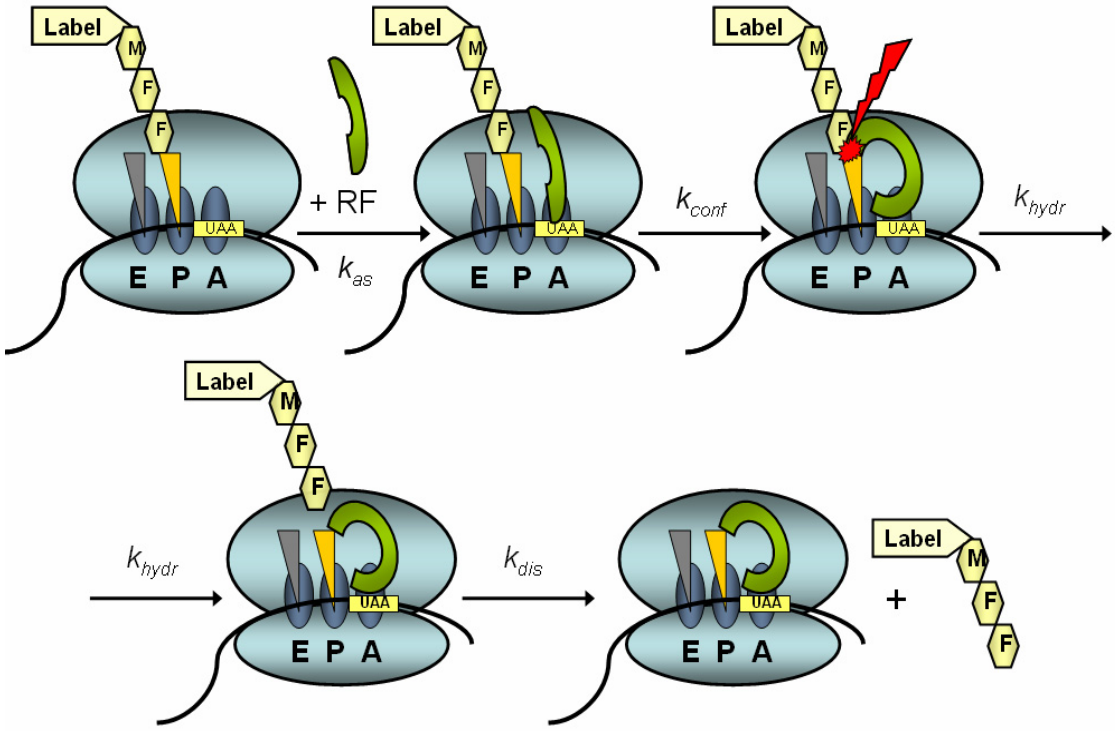

Figure 3. The sequence of events upon mixing release factors (RF) with the release complexes. Firstly, the RF binds to the ribosome with the rate $k_{as}[RF]$ proportional to the RF concentration. Then it undergoes a putative conformational change with a rate k_{conf} followed by the catalytic step with the rate k_{hydr}. The hydrolysed peptide is released from the ribosome with a rate k_{dis}. The label is radioactive ^{3}H in quench flow or fluorescent coumarin derivative in stopped flow experiments.

coumarin derivatives to fluorescently label the peptide. RCs were prepared using an in vitro translation system assembled from purified *E. coli* components. The RCs were purified from other components of the translation mixture by pelleting through a sucrose cushion (see MM).
The quality of the RCs was checked by high pressure liquid chromatography (HPLC) and the elution profiles shown in Fig. 4 demonstrate that the complexes contained around 80% the fMFF tripeptide, but also some amount of fMF dipeptide and fM that were not converted into tripeptides.

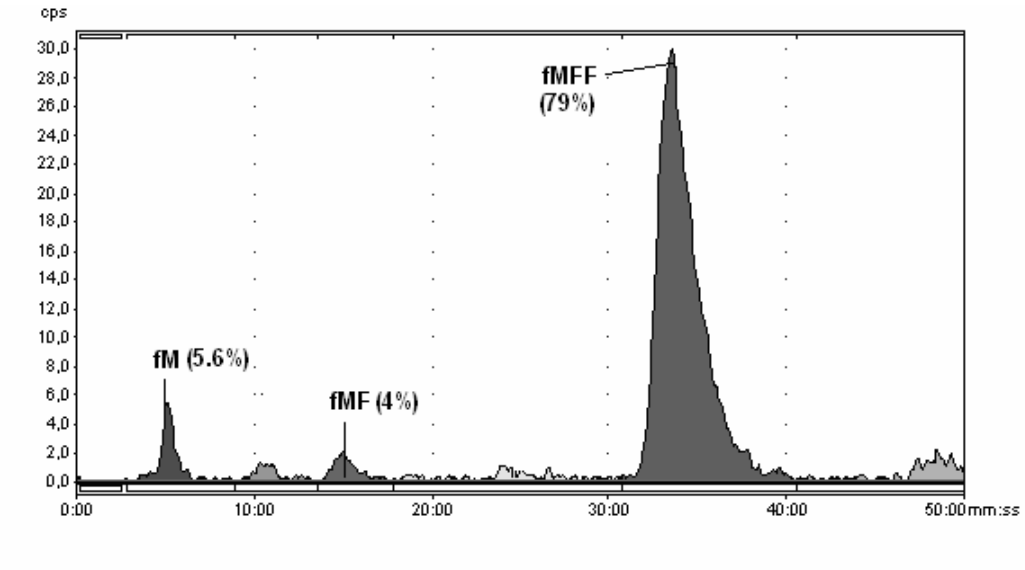

Figure 4. An HPLC elution profile of *in vitro* synthesized release complexes containing fMFF tripeptide. The majority of the ^{3H}fMet was converted into fMFF tripeptide, but there were small amounts of fMF dipeptide and fM present.

2.2. Peptide release by methylated RF1

The kinetics of MFF tripeptide release by mRF1 was studied with both quench flow (QF) and stopped flow (SF) techniques. In both these techniques the reaction is initiated by a fast mixing of two separately prepared solutions, one containing release complexes (RCs) and the other the release factors (RFs). An important advantage of SF over QF is that with this technique the whole time course of the reaction can be followed by continuously detecting fluorescence change in the reaction mixture. In contrast, in QF experiments each time point of the time course of the reaction is a result of a separate experiment in which the two solutions are mixed, allowed to react for a specified time, and the reaction is then quenched with acid. The amount of the reaction product after quenching is quantified by another method (for example, scintillation

counting or HPLC). As a result a QF experiment takes much longer time to carry out and some special measures should be taken to prevent spontaneous uncatalysed hydrolysis of release complexes, especially at high pH.

The time courses of fluorescent Cm-MFF tripeptide release by mRF1 obtained in SF experiments conducted at different pH values are shown in Fig. 5A. The rate of Cm-MFF peptide release increased with pH, but above pH 7.9 the time courses became obviously biphasic. Fig. 5B shows how the rate of the fast phase with dominant amplitude increases with pH while the rate of the slow phase of peptide release remains more or less constant. In addition to strong pH dependence Fig. 5 also demonstrates an apparent saturation of the fast release rate (k_{fast}) with increasing OH^- concentration. If we assume that the real substrate of the reaction is a hydroxide ion then the rate of the reaction should increase linearly with OH^- concentration as $k_{hydr}[OH]$.

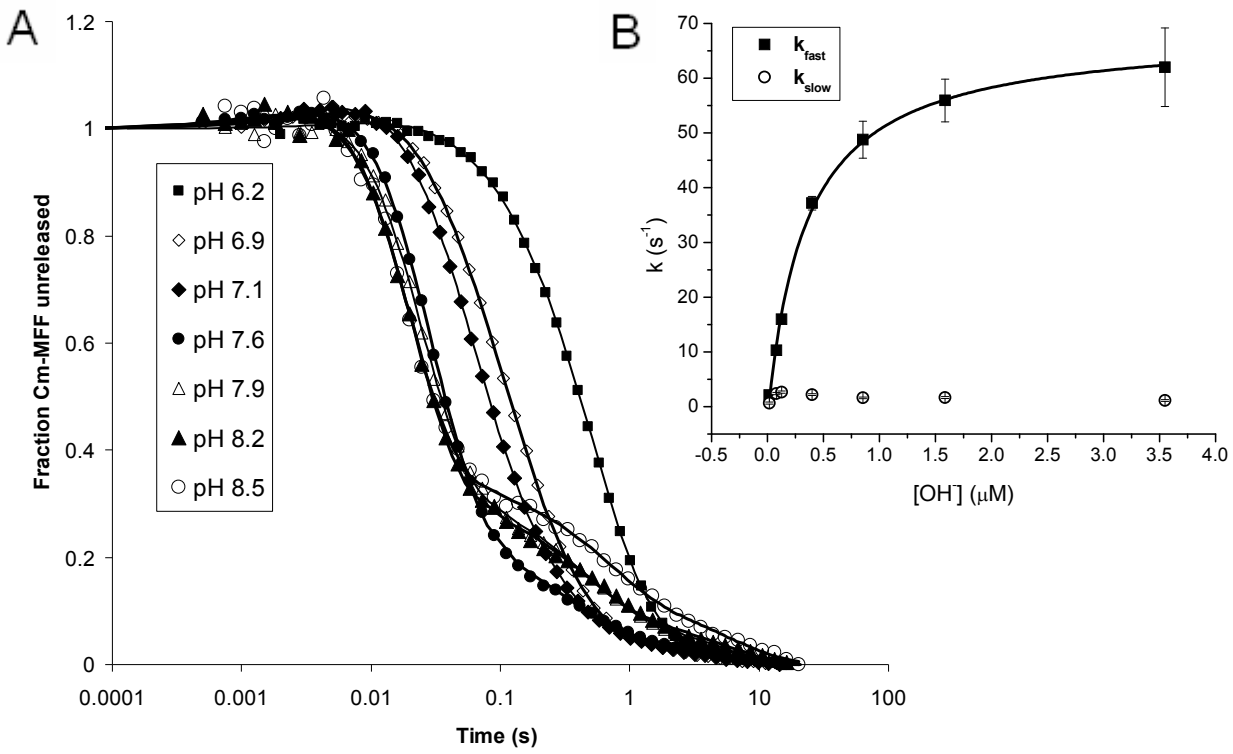

Figure 5. (A). Time courses of peptide release by methylated (wild type) RF1 at different pH values obtained with stopped flow technique. Release complexes containing ribosomes with fluorescent-labeled MFF tripeptide in the P site and UAA stop codon in the A site were reacted with saturating amounts of mRF1. (B) Dependence of the release rates on OH^- concentration in the reaction mix.

Indeed, at low pH the increase is almost linear but there is a strong deviation from linear dependence at high pH (Fig. 5B). It indicates a presence of a reaction step that precedes the chemical hydrolysis and is not affected by OH^- concentration. The average time of the release reaction should include the time of this preceding step (t_{pr}), and depend on the hydroxide ion concentration as:

$$t_{react} = t_{pr} + \frac{1}{k_{hydr}[OH]} \quad (1)$$

This dependence would explain the shape of the curve in Fig. 5B and the saturation of the reaction rate $k = 1/t_{react}$ at the value $1/t_{pr}$.

In the case of the release reaction on the ribosome t_{pr} includes at least two steps preceding the chemical step of the release (see Fig. 3). Firstly, the release factor (RF) binds to the ribosome with the rate $k_{as}[RF]$ proportional to the RF concentration. Then the RF undergoes a putative conformational change with a rate k_{conf} making it competent for catalysis. In an SF experiment we should also consider the rate of dissociation (k_{dis}) of the released peptide (see Fig. 3). This is because the major change in the fluorescence signal occurs not in the chemical step, but upon the released peptide dissociation from the ribosome. Then the total average time of the release reaction measured in the SF experiment is the sum of all these times:

$$t_{SF} = \frac{1}{k_{as}[RF]} + \frac{1}{k_{conf}} + \frac{1}{k_{hydr}[OH]} + \frac{1}{k_{dis}} \quad (2)$$

This relation shows that there are three $[OH]$-independent terms that could explain the saturation of the apparent rate of hydrolysis at high OH^- concentrations and that the conformational change in the release factor/ribosome complex after the RF binding is only one of the three.

2.3. The saturation of release rate with pH is not due to peptide dissociation

Since the main fluorescence change in the SF experiment occurs not upon the ester bond cleavage itself, but upon the dissociation of the released peptide from the ribosome, the saturation of the release rate measured by SF technique may occur when this dissociation step becomes the rate limiting one. To exclude this possibility we measured the kinetics of fMFF release with quench flow technique for which the total reaction time does not include the time of peptide dissociation:

$$t_{QF} = \frac{1}{k_{as}[RF]} + \frac{1}{k_{conf}} + \frac{1}{k_{hydr}[OH]} \quad (3)$$

The time courses obtained in QF experiments at different pH are shown in Fig. 6. As in the case of SF the kinetics measured by QF displayed a biphasic behavior with a similar distribution of the fast and slow phases. The fast rate of peptide release increased with pH (Fig. 6B) and also

showed the similar signs of saturation (compare Fig. 5B and 6B) at high pH. Therefore we concluded that the saturation of the pH dependence is not a peculiarity of the SF experiments.

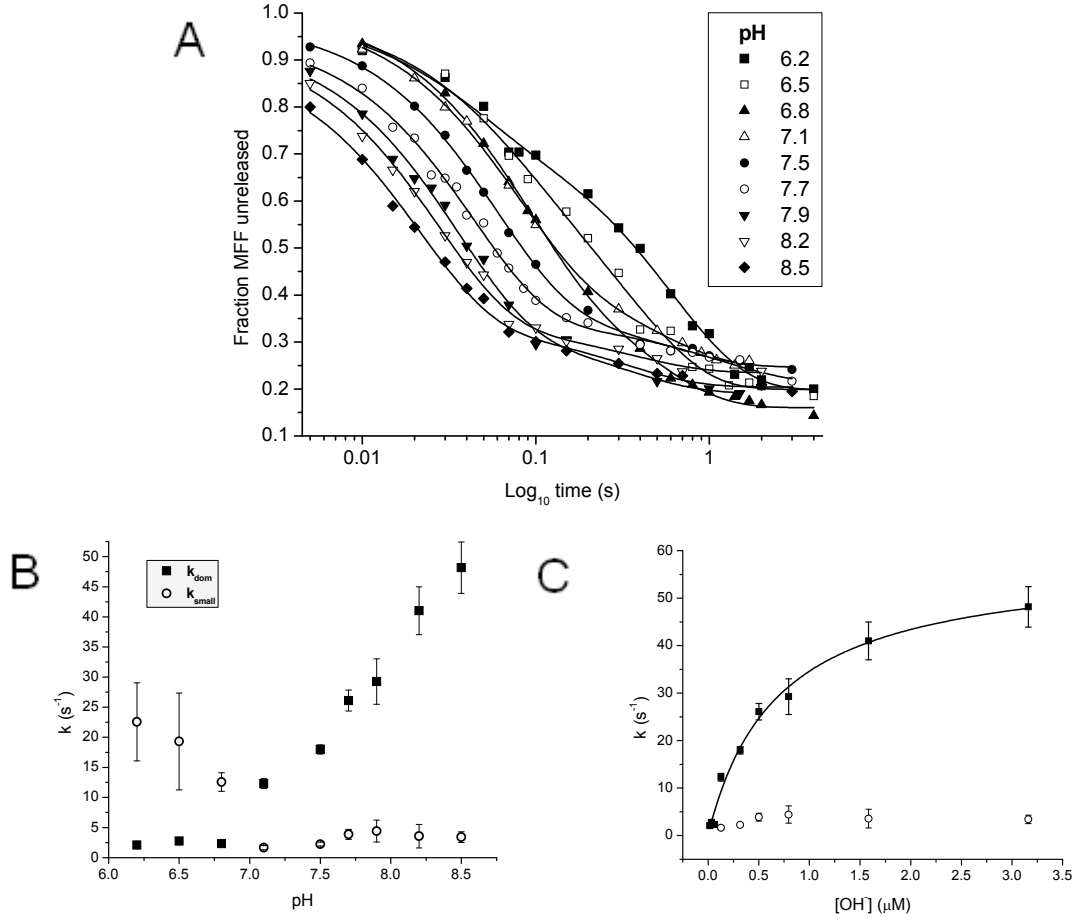

Figure 6. Time courses of peptide release by methylated (wild type) RF1 at different pH values obtained with quench flow technique (A). Release complexes containing ribosomes with ^{3H}fMFF-tRNA in the P site and UAA stop codon in the A site were reacted with saturating amounts of mRF1. B. pH dependence of the release rates on OH^- concentration it the reaction mix. Dependence of the release rates on OH^- concentration it the reaction mix is shown in C.

2.4. Discrepancy between quench flow and stopped flow methods at low pH

The SF and QF results were similar at high pH but differed in the low pH range. According to SF the fast rate with dominant amplitude of around 70-80% (the rates and amplitudes are compiled in Tables in the Appendix) decreased with decrease in pH and the slow rate was essentially pH-independent (Fig. 5). However, in all QF experiments we saw a considerable increase in the rate of the slow, non-dominant phase with decrease in pH (Fig. 6).

We concluded that one of the methods, QF or SF, gave artificial results at low pH values. Firstly, we tested if the absence of the fast rate at low pH was caused by properties of the fluorescent label. We used a different coumarin derivative, Mq (see MM), for which the fluorescence increased upon the peptide release the contrary to the Cm label used before for which the fluorescence decreased (compare Fig. 5A and Fig. 6A.) We expected that a different shape of the time curves would allow detection of the fast rate at low pH seen in QF experiments. Fig. 7 shows the time courses of Mq-fMFF peptide release by unmetlylated RF1 and methylated RF2. Comparison of Fig. 5A and Fig. 7A shows that they are almost mirror images of each other. There was one deviation from this pattern: a sharp drop of the rate of peptide release by mRF2 at pH 8.5 (Fig. 7D). It is possible that it shows a degradation of the protein at high pH. However, it was not observed with RF1 (methylated or not) and probably demonstrates that RF2 is more sensitive to pH conditions. There was no increase in release rate at low pH for any of the factors. So, we concluded that even with a different label the fast rate at low pH could not be detected in SF experiments.

Next we tested our quench flow instrument and discovered a presence of the fast release of small amplitude even without the release factor added to the reaction mixture. We have then traced the origin of this artificial fast rate to the problem of our QF instrument. Namely, for the fast time points (less that 0.07 s) the QF instrument works in the so called flow mode where the delay between the mixing and quenching is determined by the rate of the flow and the length of the loop between the mixing and quenching points. The longer time points (0.07 s and above) are taken in a so called push-and-wait mode where the reaction mix is first rapidly mixed, then allowed to age and expelled for quenching. The push-and-wait mode results in up to two-fold larger volume of the quenched sample that the flow mode. Since the amount peptidyl-tRNA per reaction is constant, the concentration of peptidyl-tRNA in the reaction samples for long time points would be two-fold lower than for the short ones. As the concentration of peptidyl-tRNA in the quenched reaction is very low this might cause differential precipitation for the reaction samples taken at long and short QF time points. This was indeed the case. The addition of a stronger precipitating agent, trichloroacetic acid (TCA), essentially eliminated the differential precipitation problem upon switching from the “flow” to “push” mode of the QF instrument and this resulted in the disappearance of the fast phase of small amplitude which persisted in our initial QF measurements (see MM for more details).

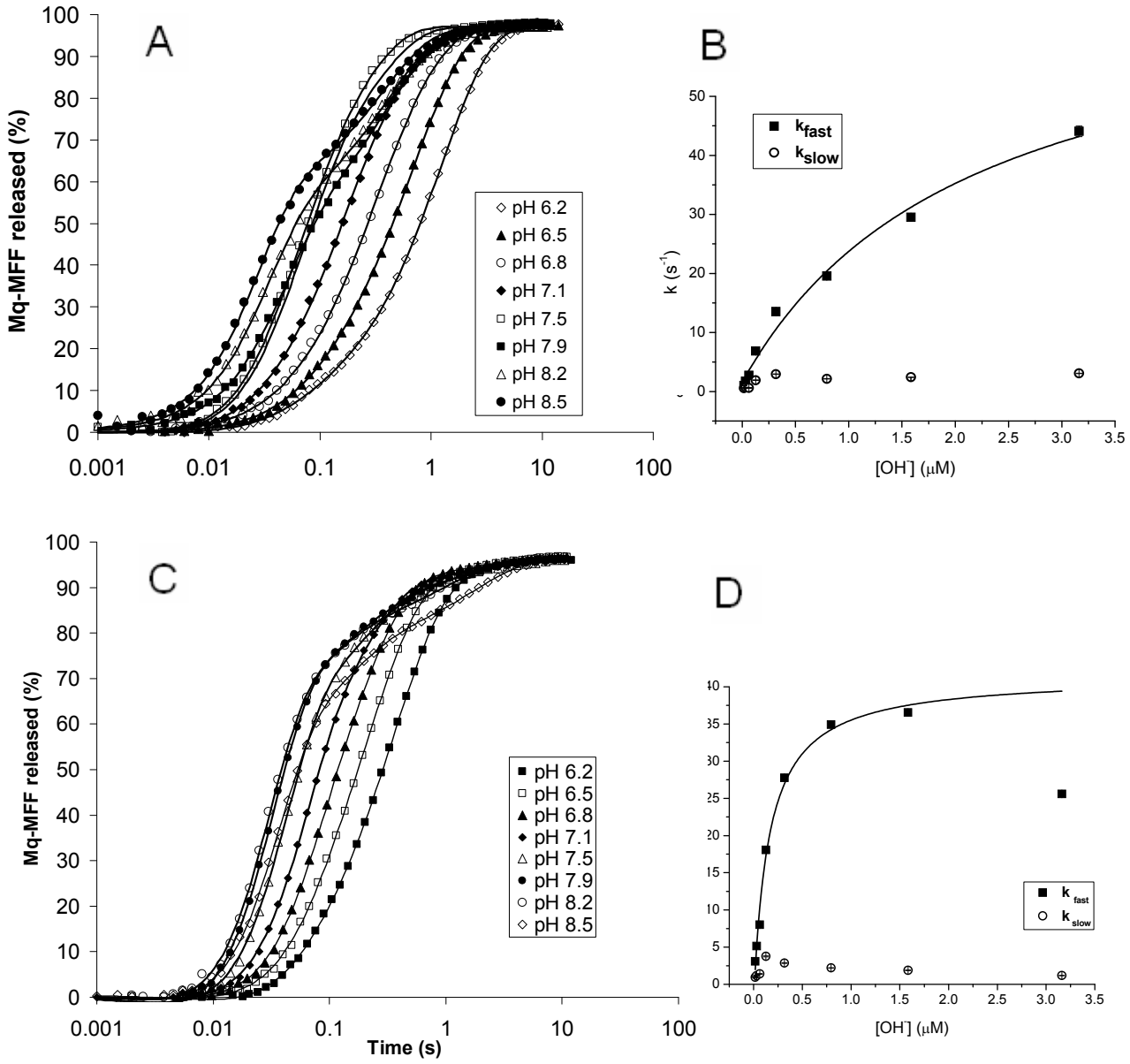

Figure 7. Time courses of peptide release by unmethylated RF1 (A) and methylated RF2 (C) at different pH values obtained with stopped flow technique. Release complexes containing ribosomes with fluorescent labelled Mq-MFF tripeptide in the P site and UAA stop codon in the A site were reacted to saturating amounts of release factors. The dependence of the release rates on OH^- concentration it the reaction mix is shown in (B) for uRF1 and (D) for mRF2.

2.5. Aminolysis does not significantly contribute to the peptide release at high pH

We also wanted to rule out the possibility that the increase of the rate of peptide release at high pH seen both in the QF and SF experiments was due to increased contribution of aminolysis. The PM buffer we use in our experiments contains high concentrations of alkyl-amines spermidine and putrescine (See MM) that could act as nucleophiles at high pH due to de-protonation of their amino groups. To check for aminolysis products we ran an RF-catalysed release of fMFF peptide at pH 8.5 and at pH 7.3 for comparison and studied the products of the reaction on HPLC. No aminolysis products were detectable in the elution profiles (Fig. 8). The composition of peaks is almost identical at pH 7.3 and 8.5 and there are no additional peaks that could contain aminolysis products. It confirms the previous results by (Shaw and Green, 2007) who had demonstrated that RFs specifically excluded large nucleophiles from the catalytic site in favour of smaller ones, such as water.

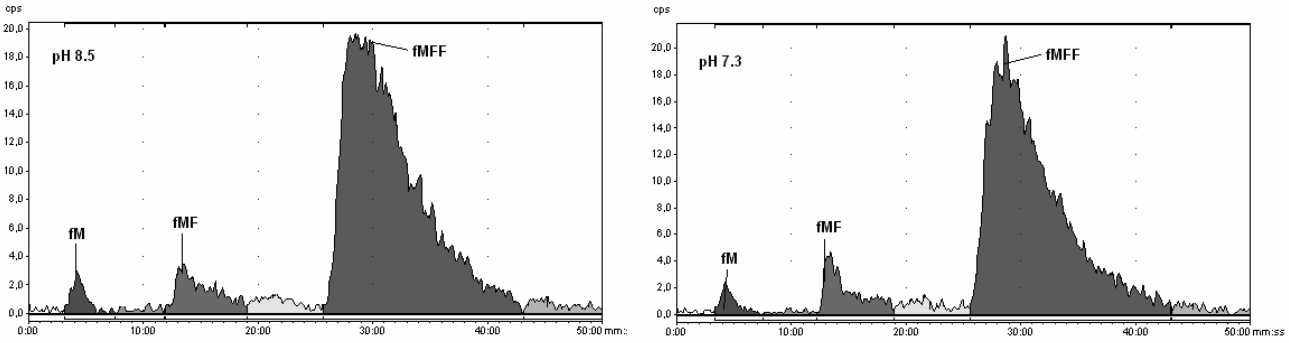

Figure 8. Elution profiles after complete release by umethylated RF1 at pH 8.5 and pH 7.3. Release complexes were incubated with saturating amounts of uRF1 for 40 s and reaction products were analyzed on HPLC.

2.6. The RF binding step can not explain the saturation of release rate.

To exclude the possibility that the saturation of the fast rates of peptide release in figures 5B, 6C, 7B and 7D was due to the slow RF binding to ribosome complexes we varied the concentration of release factor both in the SF and QF experiments. The results are summarised in Table 1. A 2-fold increase of RF concentration had no effect on termination rate both in stopped flow and quench flow. Even an 8-fold increase from 1 μM to 8 μM had small effect: the rate increased 1.2 times instead of 8 that would be expected if the experiment was performed in sub-saturating conditions. We concluded that our experimental conditions were reasonably close to the so called k_{cat} range where the reaction rate is not affected by the step of RF binding to the ribosome (k_{as}).

Table 1. Release rates measured at different concentrations of unmethylated RF1.

Release factor (method)	pH	Release factor concentration (μM)	Release complex concentration (μM)	k_{fast} or k_{dom} (s^{-1})
uRF1 (Stopped flow)	7.5	2	0.02	12.90±0.004
	7.5	4	0.02	12.38±0.003
	7.7	1	0.02	16.56±0.007
	7.7	8	0.02	19.69±0.005
mRF1 (Quench flow)	7.9	2	0.01	29.26±3.77
	7.9	4	0.01	33.06±5.56

2.7. The nature of the slow phase of peptide release.

The time courses of peptide release were biphasic in all our experiments. There was a dominant pH-dependent fast phase and a slow pH-independent phase with low amplitude (see Appendix for the percentage of amplitudes). We originally ran the release experiments with methylated release factors RF1 and RF2 produced in the strains with over-expressed methylating enzyme (Heurgue-Hamard et al., 2002). Methylation is known to considerably increase the rate of peptide release in the case of RF2 (Dincbas-Renqvist et al., 2000) and we interpreted the presence of slow phase of peptide release in experiments in Fig. 5 as being due to some fraction of unmethylated RF1 or RF2 in our RF preparations. However, the results of experiments in Fig. 7B where we studied the pH dependence of the rate of release with unmethylated RF1 argue against this interpretation. The fraction of slow and fast phases of release was very similar with methylated and unmethylated versions of RF1. Therefore, the slow phase in peptide release can not be a consequence of the presence of methylated and unmethylated RF forms in the factor preparations. Moreover, the effect of methylation on RF1-catalysed release was much smaller than that reported in the case of RF2.

Another possible origin of the slow phase could be the erroneous termination on the sense codon. Indeed, Fig. 4 shows that our release complexes contained a considerable fraction of fMF dipeptide. Fig. 8 shows that the incubation with release factors resulted in the release of the dipeptide as well. The complexes containing fMF dipeptide presumably contained a Phe codon UUC in the A site and the release of fMF could occur because of erroneous termination on this codon. To study this possibility we prepared fMFF complexes containing the most error prone sense codon UGG (Freistroffer et al., 2000) in the A site and studied the rate of release of fMFF peptide in a standard QF release experiment. The result of a series of release experiments

presented in Fig. 9 show that the rate of release, 0.03 s^{-1} of MFF tripeptide on the UGG sense codon was much too slow to explain the slow phase (with the rate of about 2 s^{-1}) observed in our previous pH experiments. We concluded that the release on the sense codon can not explain the presence of the slow phase of release seen both by QF and SF experiments at high pH values. We further discuss the possible origin of the slow phase in the "Discussion" section.

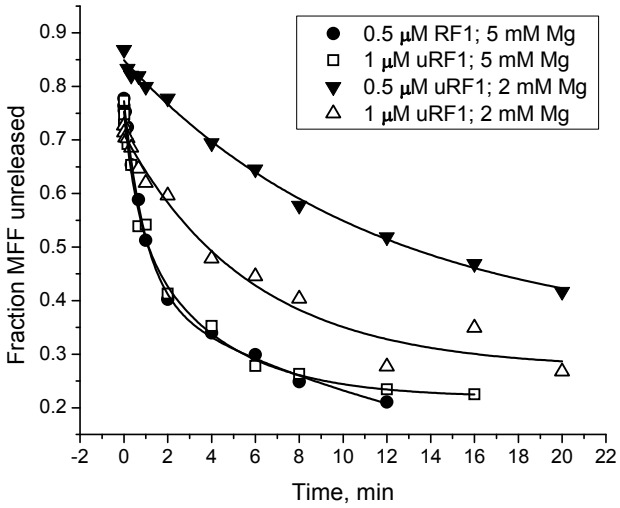

Figure 9. The time courses of peptide release on UGG codon at different concentrations of unmethylated RF1 and free Mg obtained by quench flow.

2.8. Magnesium dependence of erroneous peptide releases

Interestingly, the rate of release we measured on UGG codon was much faster than reported previously (Freistroffer et al., 2000). It was not affected by the decrease in RF1 concentration (Fig. 9) indicating that our experiments were conducted in k_{cat} range of RF concentrations and that the estimated values of k_{cat}/K_M represent the low bound of the k_{cat}/K_M parameter. This also implies that the actual k_{cat}/K_M value must be higher than 0.03 $\mu M^{-1}s^{-1}$ and almost 20-fold higher than reported previously (Freistroffer et al., 2000). One reason for the inconsistency with the previous results could be the high Mg concentration (5 mM) used in our release experiments to stabilise the ribosomes in vitro. Indeed, the decrease of Mg concentration to a more physiologic 2 mM used previously (Freistroffer et al., 2000) decreased the rate of fMFF peptide release almost 10-fold. It has also brought us back into the k_{cat}/K_M range of RF1 concentrations since the decrease in the RF1 concentration from 1 to 0.5 μM resulted in almost 2-fold (from 0.0026 to 0.0015 s^{-1}) decrease in the rate of peptide release on the UGG codon. We

used these data to get a reliable estimate of k_{cat}/K_M parameter as 0.003 $\mu M^{-1}s^{-1}$ for unmethylated RF1 at 2 mM Mg in the reaction mixture. The value reported by (Freistroffer et al., 2000) was 0.0018 $\mu M^{-1}s^{-1}$. Taking into account that we used release complexes with fMFF-tRNA instead of fMFTI-tRNA and unmethylated RF1, our results are in reasonable agreement with their findings. As the k_{cat}/K_M value for cognate reaction is about 60 $\mu M^{-1}s^{-1}$ (Freistroffer et al., 2000), the accuracy of RF1 in discriminating against UGG codon is about 20,000 - a value normally associated with the accuracy of aminoacyl-tRNA selection by the ribosome (Johansson et al., 2012). These experiments also show that like the selection of aminoacyl-tRNA by the ribosome the accuracy of termination is also sensitive to Mg concentration in the reaction mixture. The decrease in the accuracy of termination with increase in Mg concentration is probably due to increased binding of RF to the ribosome.

3. Discussion

3.1. pH dependence of termination

Our results in Fig. 5 and Fig. 7 show that with methylated RF1 or RF2 the rate of peptide release from the ribosome is about 20 s^{-1} at physiological pH values but it increases up to 70 s^{-1} at high pH in the reaction mixture. Therefore one can conclude that the rate of peptide release is suboptimal under in vivo conditions. On the other hand, it should be kept in mind that it takes about 20 s to synthesize an average protein in the *E. coli* cell. So, the time of termination in vivo (50 ms = 1/20 s^{-1}) contribute only a tiny fraction (<0.3%) to the total synthesis time. It means that the pH dependence of the rate of peptide release has little if any physiological significance. However, it has implications for the mechanism of peptide release reaction on the ribosome.

It has been often remarked that both the peptide release and the peptidyl transfer reactions on the ribosome are chemically similar (Brunelle et al., 2008; Green and Lorsch, 2002) representing two cases of nucleophilic reactions (hydrolysis and aminolysis) where a nucleophile (water or amine) attacks the carbonyl carbon of the ester bond in the peptidyl-tRNA. The pH dependence of peptide release reaction was recently observed by (Kuhlenkoetter et al., 2011). The pH dependence of the peptidyl transfer reaction has been observed in a recent study with natural substrates (Johansson et al., 2011) and in a number of earlier ones with artificial substrates (Beringer and Rodnina, 2007; Katunin et al., 2002). Therefore, the strong pH dependence of the release reaction reported in this study does not come as a surprise. However, despite apparent similarity there are also some important differences between the two reactions. In the case of peptidyl transfer reaction, the nucleophile is an NH_2 group that loses its nucleophilic properties when protonated. Thus, the pH dependence of the peptidyl transfer reaction is expected to tightly follow the course of NH_2 de-protonation and to have a well defined and easily explainable pK value (Johansson et al., 2011). In contrast, in the case of peptide release, both the water molecule and the hydroxide ion (OH^-) are nucleophiles with available lone electron pairs of the oxygen. Moreover, with the exception of the work by (Kuhlenkoetter et al., 2011), almost all reaction schemes of peptide release postulate water, not hydroxide, to be the nucleophile in the hydrolytic reaction despite the fact that hydroxide ion is a much stronger nucleophile. The pH dependence of the rate of peptide release, therefore, is a really surprising observation in context of the reaction mechanisms of peptide bond hydrolysis by RFs proposed so far. Neither of the schemes suggested in crystallographic studies (Jin et al., 2010; Korostelev, 2011; Song et al., 2000) or in theoretical studies (Trobro and Aqvist, 2009) include catalytic groups or substrates that become protonated or deprotonated in the pH range from 7 to 8.

Indeed, if we look at Fig. 10A which corresponds to the reaction scheme proposed in (Jin et al., 2010) it is obvious that here a hydroxide ion can not replace a reactive water molecule. This is because the amide oxygen of Gln is the acceptor of hydrogen bond from water and has a partial negative charge which would repel the negatively charged hydroxide ion as is shown in Fig. 10B. However, if the amide group is of Gln is flipped as shown in Fig. 10C, then the hydroxide ion can be accommodated easily in place of water and stabilized by the amino group of the amide that now donates a hydrogen bond. The possibility that a hydroxide ion is the substrate in the release reaction was suggested in (Kuhlenkoetter et al., 2011) (Fig. 2c in this article). An alternative reaction scheme in (Kuhlenkoetter et al., 2011) (Fig 2d in this article) in which the hydroxide ion just catalyses the reaction by abstracting a proton from the reactive water molecule is in a sense equivalent to the direct participation of hydroxide ion, since a proton transfer is not

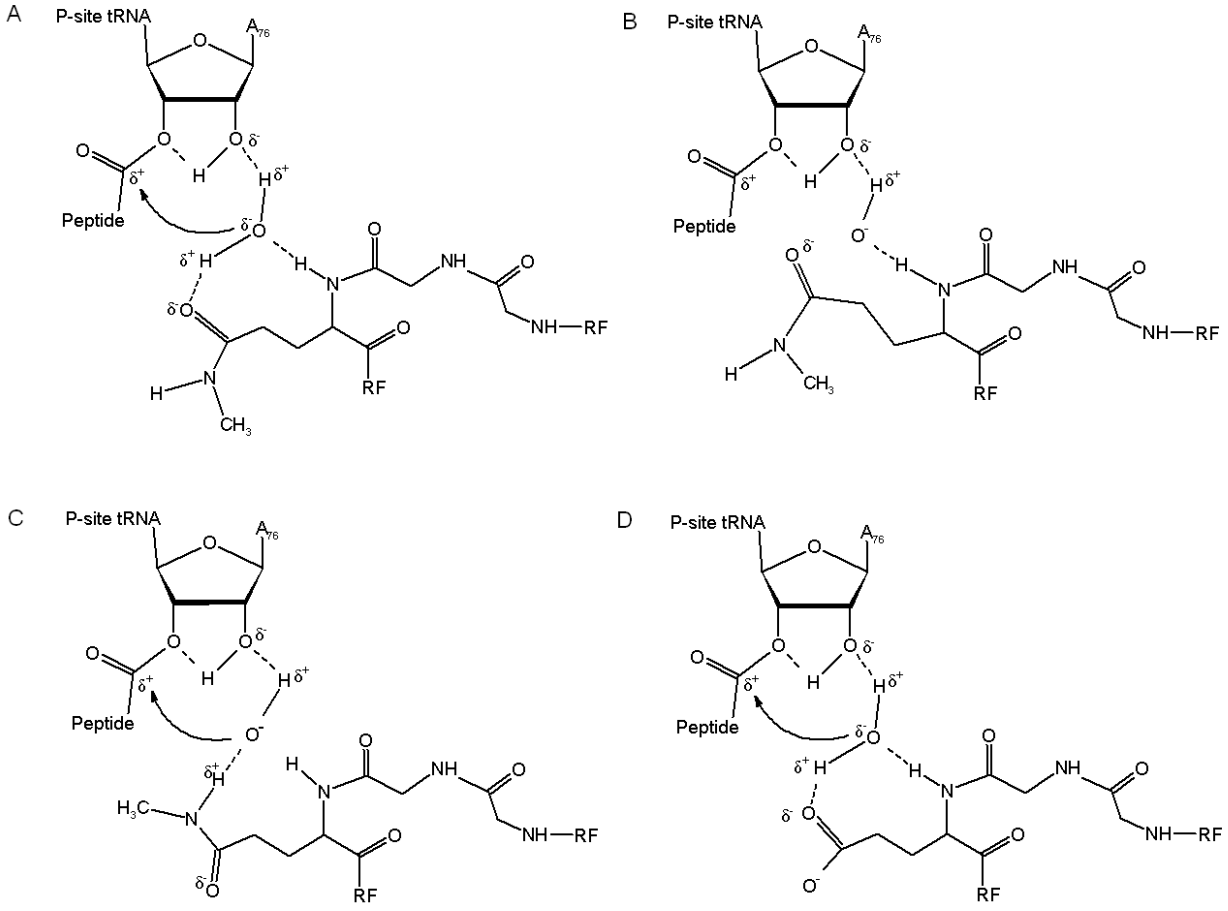

Figure 10. Different reaction schemes of RF-catalyzed hydrolysis of the ester bond between the nascent peptide and the tRNA in the P site. (A) shows a mechanism involving water as a nucleophile proposed by Jin et al. (2010). (B) shows that the same mechanism would not be possible with a hydroxide ion as a nucleophile because the amide oxygen of Gln would repel the negatively charged OH^-. (C) shows how the OH^- ion could be accommodated by Gln amide group. (D) shows a reaction mechanism involving glutamic acid instead of glutamine.

rate limiting. The presence of a slow phase with pH-independent rate of peptide release might be explained by the existence of two configurations of the GGQ motif that differ in the orientation of the amide of the reactive Gln (see Fig. 10A and Fig. 10C). If 20% of RF contains amide oriented for the water reaction and 80% oriented for the hydroxide reaction this would result in 80% of pH dependent and 20% of pH independent peptide release. To test this hypothesis we are going to prepare a mutant RF2 with the glutamine residue replaced by glutamic acid that does not have an amide group on its side chain and would not be able to coordinate an OH^- ion. If our model is correct, the peptide release of the mutant RF2 should be pH-independent and follow the reaction scheme presented in Fig 10D.

3.2. Rate limiting steps in peptide release

The shape of pH dependence of the peptide release rate in Figures 5-7 indicates the presence of a rate limiting step largely independent on hydroxide ion concentration in the reaction mixture. The comparison of results obtained by QF and SF techniques excludes the possibility that the dissociation of peptide from the ribosome after its release is the rate limiting step that causes saturation in SF experiments. Moreover, the small effect of large variations in RF concentration on the rate of release measured both by the QF and SF techniques demonstrates that the release reaction is in the k_{cat} range of release factor concentrations. It means that RF concentration in our experiments is high enough to make the RF binding to the ribosome not rate limiting for the release reaction. This leaves a conformational step preceding the hydrolytic reaction as the most probable explanation for the observed hyperbolic dependence of the release rate on the OH- concentration. The nature of this putative conformation step has been discussed in a recent review by (Korostelev, 2011). It may represent the change in the angle between the anticodon arm and the GGQ arm of RF that occurs in response to the stop codon recognition and allows the GGQ motif to enter the PTC of the ribosome while the RF maintains the contact with the stop codon in the A-site. The hinge between these two arms of RF is certainly flexible because the RFs can acquire different conformations in a solution and on the ribosome (Korostelev, 2011). This induced fit mechanism could also contribute to a very high accuracy of the release observed earlier (Freistroffer et al., 2000) and confirmed here by experiments in Fig. 9.

3.3. Role of glutamine methylation

As it was mentioned in the introduction, the amide of glutamine residue in the GGQ motif is N-methylated in vivo (Dincbas-Renqvist *et al*., 2000). Inactivation of PrmC methyltransferase that methylates release factors in *E .coli* results in a slow growth phenotype, but is not lethal (Nakahigashi et al., 2002). In vitro the unmethylated RF2 is about 10 times slower when

releasing a dipeptide, but only 5 times slower in tetra-peptide release (Dincbas-Renqvist *et al.*, 2000). Our results indicate that in the case of RF1 methylation has only a modest effect. The k_{cat} was reduced less than 2-fold when releasing a tripeptide. Moreover, methylation did not qualitatively affect the pH dependence of the release reaction. The presence of the pH-dependent fast phase and its saturation at high pH and pH-independent slow phase of the peptide release were seen with both methylated and unmethylated RF1. Methylation of the Gln side chain probably stabilises the position of the Glu side chain in the PTC (Trorbo, Aqvist 2007). One can conclude that Q-methylation is important only for the fine tuning of the release reaction in the case of RF1 but probably plays a much more important role for RF2.

3.4. Conclusions

We have shown that hydrolysis of the ester bond between peptide and tRNA in the P-site of the ribosome by class I release factors is strongly pH dependent. The rates we measured of releasing a tripeptide were higher that the rates of fMet peptide mimic release reported previously. We determined that the rate of release becomes saturated at high pH values and that could indicate a fast conformational step on the reaction pathway that precedes the chemical reaction of the ester bond hydrolysis. We also demonstrate how these results could be compatible with a reaction scheme where a hydroxide ion, not a water molecule, participates in the ester bond hydrolysis. We have also shown that both stopped flow and quench flow methods may be complementary for future studies of termination if the difference between the two modes of quench flow action is taken into account.

4. Materials and methods

4.1. Chemicals and Buffers

Radioactive [^{3}H] methionine was from GE Healthcare. The fluorescent modified coumarine labels methoxy-coumarin (Cm) and aminomethyl-coumarin (Mq) were from Invitrogen. Phosphoenolpyruvate (PEP), pyruvate kinase (PK), myokinase (MK), inorganic pyrophosphotase (PPi), spermidine, putrescine, non-radioactive amino acids were from Sigma-Aldrich. Ribolock RNAse inhibitor was from Fermentas. All other chemicals of analytical grade were from Merck.

All experiments were carried out in a polymix-like (PM) buffer (Jelenc and Kurland, 1979) containing 5 mM $Mg(CH_3COO)_2$, 95 mM KCl, 3 mM NH_4Cl, 0.5 mM $CaCl_2$, 30 mM 4-(2-hydroxyethyl)-1-piperazineethanesulfonic acid (HEPES), 1 mM spermidine, 8 mM putrescine and 1 mM 1,4-dithioerythritol (DTE). When needed the pH was adjusted with 0.5 M KOH or 1 M HCl. Where indicated, the concentration of Mg^{2+} ions was increased with $Mg(CH_3COO)_2$ or decreased by adding GTP since it chelates one Mg^{2+} ion per GTP molecule.

4.2. Preparation of fluorescent-labelled Met-tRNA^{Met}

4.2.1. Charging of tRNA^{Met}

Charging mix (2 ml total) contained 150 µM ^{3}H-labelled Met, 80 µM tRNA^{Met}, 0.3 units Met-tRNA^{Met} synthetase, 2 mM $Mg(CH_3COO)_2$, 2 units PK, 1 unit MK, 1 µM PPi, 400 units Ribolock, 2 mM ATP, 20 mM PEP, 1 mM DTE, 30 mM HEPES. The tRNA was charged for 30 min at 37°C and phenol/chisam extraction was performed. Equal volumes of phenol pH 5.4 and chisam (24:1 chloroform/isoamyl alcohol vol/vol) were added and the mix was incubated for 5 min at room temperature and vortexed periodically during this time to keep the aqueous and organic solvent phases well mixed. Then the mix was centrifuged at 20817 x g for 10 min at 4°C to separate the aqueous and organic layers. The top aqueous layer was collected and ethanol precipitated with 1/10 volume of 3 M CH_3COONa and 2.5 volumes of 95% ethanol for 5 min at -80°C and then for 30 min at -20°C. The solution was centrifuged at 20817 x g for 15 min at 4°C and the supernatant discarded. The pellet was washed with 80% ethanol, centrifuged at 20817 x g for 5 min at 4°C and the supernatant discarded. The pellet was dissolved in ddH_2O and CH_3COONa added to 0.1 M.

4.2.2. Modification of Met-tRNA^{Met} with a fluorescent label

The charged Met-tRNA^{Met} was modified with a fluorescent label. 6 mg of Mq or Cm was prepared in 1.2 ml DMSO and 0.5 ml of the mix was added to 0.3 ml of Met-tRNA^{Met}. The solution was incubated for 1 hour, then the rest of Mq or Cm added and NaCl added to the concentration of 100 mM. The reaction mix was kept in the dark at 4°C overnight. The next day it was ethanol precipitated to remove DMSO and not reacted Mq or Cm, extracted twice with phenol/chisam and ethanol precipitated again. The pellet was dissolved in ddH_2O.

4.2.3. Purification and concentration of fluorescent-labeled Met-tRNA^{Met}

Mq- or Cm-labeled Met-tRNA^{Met} was purified on a HPLC system (Waters) equipped with UV and fluorescent detectors to separate it from non-charged or non-modified tRNA. Cm-Met-tRNA^{Met} or Mq-Met-tRNA^{Met} was eluted using a linear gradient from 60% buffer A [20 mM CH_3COONH_4 pH 5.0; 5 mM $MgCl_2$; 400 mM NaCl] and 40% buffer B [buffer A in 40% methanol] to 10% buffer A and 90% buffer B and collected using a fraction collector (FRAC-100, Pharmacia). Both UV (260 nm) and fluorescence (Cm: excitation at 380 nm, emitation at 470 nm; Mq: excitation at 360 nm, emitation at 410 nm) signals were monitored. 10 µl of fractions corresponding to the peak of both UV and fluorescence were counted in Quicksafe Flow 2 scintillation liquid in Beckman Coulter LS 6500 counter to confirm the presence of charged tRNA. Fractions containing most radioactivity were pooled together and concentrated in 10 kDa cutoff centrifugal filters (Amicon). The concentration of purified Mq-Met-tRNA^{Met} was estimated by dividing counts per 1 min per 1 µL by specific activity of ^{3}H-labelled Met and was 72 µM. The concentration of purified Cm-Met-tRNA^{Met} was 26 µM.

4.3. Purification of 70S ribosomes

4.3.1. Opening of the cells

70S ribosomes were purified from *E. coli* strain MRE 600, using sucrose gradient zonal ultracentrifugation as described (Rodnina and Wintermeyer, 1995). 70 g of frozen *E. coli* MRE600 cells were slowly thawed at 4°C by stirring in 70 ml of cell opening buffer [20 mM Tris-HCl pH 7.5 , 100 mM NH_4Cl , 10 mM $Mg(CH_3COO)_2$, 0.5 mM EDTA, 3 mM β-mercaptoethanol]. After thawing 0.2 ml of 1 mg/ml DNAse was added and the cells opened in a bead machine (Bead Beater, Biospec). Cell debris was spun down for 45 min at 42500 x g (Thermo Scientific Sorvall RC6+ centrifuge, F21S rotor).

4.3.2. Purification through sucrose cushions

After centrifugation supernatants were carefully removed and pooled together. 11 ml aliquots were transferred to ultracentrifuge tubes with 11 ml 1.1 M sucrose cushion in a buffer containing 20 mM Tris-HCl pH 7.5, 0.5 M NH_4Cl, 10 mM $Mg(CH_3COO)_2$, 0.5 mM EDTA, 3 mM β -mercaptoethanol. They were centrifuged for 20 h at 252500 x g at 4°C (Beckman Coulter, Optima 100 ultracentrifuge, Ti50.2 rotor) to pellet 70S ribosomes. 50S subunits were also pelleted at this stage. After centrifugation the tubes were cooled on ice, the supernatants discarded and each pellet quickly washed with 5 ml of high salt washing buffer (HSB) containing 20 mM Tris, 500 mM NH_4Cl, 10 mM $Mg(CH_3COO)_2$, 0.5 mM EDTA, 7 mM β-mercaptoethanol. Each pellet was dissolved in 3 ml of HSB, they were pooled and the volume increased to 44 ml with HSB. They were centrifuged for 10 min at 229520 x g (Beckman Coulter, Optima 100 ultracentrifuge, Ti50.2 rotor) and the supernatants pooled. 11 ml aliquots were transferred to ultracentrifuge tubes with 11 ml 1.1 M sucrose cushion. The samples were centrifuged again for 20 h at 252472 x g 4°C (Beckman Coulter, Optima 100 ultracentrifuge, Ti50.2 rotor). Next the tubes were cooled on ice, the supernatants discarded and each pellet quickly washed with 5 ml overlay buffer (OB) containing 20 mM Tris-HCl pH 7.5, 60 mM NH_4Cl , 5.25 mM $Mg(CH_3COO)_2$, 0.25 mM EDTA, 3 mM β-mercaptoethanol, dissolved in the 3 ml of OB, pooled together, the volume increased to 40 ml with OB and the concentration of sucrose increased to 2.5% by adding 40% sucrose in OB.

4.3.3. Zonal centrifugation

The 70S ribosomes were isolated by zonal centrifugation on a convex exponential gradient from 10% to 37% sucrose (1.4 L) in OB. The reo-gradient rotor (Beckman Ti15 rotor) was loaded in a following order. 400 ml OB was pumped into the rotor at 20 ml/min. After loading 200 ml the flow was reversed to let air bubbles to come out of loading tubing and then the loading continued until 400 ml of OB were pumped in. Then the 40 ml of ribosome solution were slowly loaded (at less than 5 ml/min) avoiding air bubble formation, followed by the sucrose gradient at 30-40 ml/min. Gradient bottles were on ice with 680 ml of 10% sucrose in OB in the sealed mixing chamber and 1300 ml of 40% sucrose in OB in the other chamber. The gradient was pumped until 100 ml of overlay came out from the rotor. Next 100 ml of 50% sucrose in OB was loaded at 30 ml/min (100 ml more of the overlay came out from the rotor). The pump was disconnected; the rotor sealed with a sealing cap and centrifuged for 8 h at 102000 x g at 4°C (Beckman Coulter, Optima 100 ultracentrifuge, Ti15 rotor) with acceleration and deceleration set to the slowest values. Next the gradient was pumped out of the rotor at 20 ml/min. The pump outlet was connected to an UV-unit (UV-1, Pharmacia) and the gradient was collected

in 10 ml fractions using FRAC-100 fraction collector (Pharmacia). The collection was continued until both 70S and 50S peaks were collected. The fractions belonging to the 70S peak were pooled, their volume adjusted to 200 ml with OB and the 70S ribosomes were pelleted by centrifuging for 36 h at 193280 x g at 4°C (Beckman Coulter, Optima 100 ultracentrifuge, Ti 50.2 rotor). The pellets were dissolved in total 7 ml PM, shock-frozen in liquid nitrogen and stored in aliquots at -80°C. Ribosome concentration was determined from absorption measurements at 260 nm on the basis of 23 pmol/A260 unit.

4.4. Preparation of mRNAs

4.4.1. Preparation of double-stranded DNA templates

Synthetic mRNA, encoding fMet-Phe-Phe (with UUC as Phe codon) tripeptide with a strong Shine-Dalgarno sequence was prepared by in vitro run-off transcription (Pavlov *et al*., 1997) from double stranded DNA constructs prepared with Klenow polymerase (USB). The transcription mix (1 ml) contained 7 μM of each forward and reverse DNA template, 5 μM of TritonX-100, 1 mM of each HEPES, DTE, spermidine and $Mg(CH_3COO)_2$. The mix was heated to 90°C for 15 min, allowed to air-cool slowly and cooled on ice for 5 min. Then 20 μl of dNTP mix [25 mM of each ATP, UTP, CTP, GTP] and 40 units of Klenow polymerase were added. After 1 hour of incubation at 37°C 30 units of Klenow polymerase and 20 μl of the dNTP mix were added and incubated for 1 more hour at 37°C. The mixture was extracted twice with chisam/phenol pH 8.1 in the same way as in "Charging of $tRNA^{Met}$ " and ethanol precipitated with 1/10 volume of 3 M CH_3COONa and 2.5 volumes of 95% ethanol overnight at -20°C. Next day it was centrifuged for 20 min at 20817 x g at 4°C, the supernatant discarded, pellets washed twice with 80% ethanol and dissolved in ddH_2O.

4.4.2. In vitro transcription

The standard reaction mixture (5 ml) for the *in vitro* transcription contained 40 mM Tris (pH 8.1), 6 mM $MgCl_2$, 5 mM DTE, 1mM spermidine, 4.4 mM each ATP, UTP, CTP and GTP, 1500 pmol of double stranded DNA templates, 15 units of PPiase, 0.01% (v/v) TritonX-100, 100 units of Ribolock and 2000 units of T7 RNA polymerase. The reaction mixture was incubated for 3 hours at 37°C before purification.

4.4.3. Purification and concentration of synthetic mRNA

The mRNA transcripts contained 3' poly-A tail and were purified on a poly-dT column (GE Healthcare). After the reaction had finished, the transcription mixture was diluted with TEN buffer [20 mM Tris, pH 7.5, 500 mM NaCl, 0.5 mM EDTA] and applied to a poly-dT column equilibrated with the same buffer at about 40 ml/h. After the application, the column was washed extensively with buffer TEN at 100 ml/h. The mRNA was eluted with TEN buffer without NaCl at 40 ml/h. The eluted mRNA was concentrated with 10 kDa cutoff centrifugal filters (Amicon Ultra-15 Centrifugal Filter Devices). The filters were centrifuged at 2438 x g for 25 min at 4°C (Eppendorf 5820R centrifuge; A-4-81 swing-bucket rotor), 7 ml of ddH2O added to each filter and centrifuged again at the same conditions. The quality of mRNA was checked in dipeptide formation as described in "Preparation of release complexes", except that no EF-G was added and the elution condition was 42% methanol and 0.1% trifluoretic acid, running time 20 min.

4.5. Preparation of release complexes

4.5.1. In vitro translation

Release complexes (RC) were prepared in the absence of release factors (RF) and contained the ribosomes stalled with an mRNA stop codon UAA in the A site and a tripeptidyl-tRNA with ^{3}H labelled fMet-Phe-Phe (MFF) tripeptide in the P site. They were prepared in the following way. The ribosome mix (1 ml total) was prepared in PM buffer and contained 2 μM 70S ribosomes, 3.5 μM ^{3}H labelled fMet-tRNA^{fMet}, 3.5 μM MFF-mRNA, 1 mM GTP, 1 mM ATP, 2 mM PEP, 2 μM of initiator factors IF1, IF2, IF3 and additional 2 mM $Mg(CH_3COO)_2$. The factor mix (1 ml total) prepared in PM buffer contained 10 μM EF-Tu, 1 μM EF-Ts, 3.4 μM EF-G, 5 μM tRNA^{Phe}, 0.2 mM Phe, 1 unit Phe-tRNA^{Phe} synthetase, 1 mM GTP, 1 mM ATP, 2 mM PEP, 0.5 mM DTE, additional 2 mM $Mg(CH_3COO)_2$, 1 unit PK, 100 unit Ribolock. Both mixes were pre-incubated for 20 min at 37°C, reacted together for 40 s at 37°C and cooled on ice to stop the reaction. Mg^{2+} concentration was increased by 4 mM with $Mg(CH_3COO)_2$. Fluorescent RCs were prepared in the same way except that Mq- or Cm-labelled Met-tRNA^{fMet} was used instead of f[^{3}H]Met-tRNA^{fMet}.

4.5.2. Purification on sucrose cushions

RCs were purified by sucrose gradient ultracentrifugation. Sucrose cushions contained 1.1 M sucrose in PM with 4 mM additional $Mg(CH_3COO)_2$. 500 μL of reaction mix was transferred to each ultracentrifuge tube on 500 μL of cushion and centrifuged in a swing-out rotor (S55S,

Sorvall) at 258 826 x g for 3 hours at 4°C in a Sorvall RC M150 GX ultracentrifuge. The supernatants were discarded, each pellet quickly washed with ice-cold PM, dissolved in 150 µl ice-cold PM and pooled together. RC concentration was quantified by scintillation counting in Quicksafe Flow 2 scintillation liquid in Beckman Coulter LS 6500 counter. Purified RCs were shock-frozen in liquid nitrogen and stored at -80°C.

4.5.3. Analysis by HPLC

The quality of purified complexes was analysed on a HPLC system (Waters) with online scintillation counter (βRAM3, INUS Inc.). 0.2 uM of RCs were reacted with 4 uM of RF1 at 37°C for 40 s to fully release the tripeptide and quenched with 50% FA to a final concentration of 17%. For control the same was done without RF. The samples were put on ice for 5 min to precipitate peptidyl-tRNA and then centrifuged for 15 min at 20817 x g at 4°C. The supernatants containing released peptide were applied to HPLC. The pellets containing unreleased peptide as peptidyl-tRNA were dissolved in 120 µL of 0.5 M KOH by incubating at 37°C for 10 min to hydrolyse peptide from tRNA. They were precipitated again with 20 µL of 100% FA, put on ice for 5 min and centrifuged for 15 min at 20817 x g at 4°C to pellet tRNA and other components of the reaction mixture. The supernatant containing peptide previously attached to tRNA was applied to HPLC. The sample composition was analyzed using a C18 column (Merck). The column was equilibrated with an H_2O buffer containing 46% methanol and 0.1% trifluoroacetic acid. The sample was eluted in the same buffer at 0.45 ml/min for 50 min. Over 80% of the peptide was MFF, but small amounts of MF and M were present. With RF over 80% of MFF was released. No release was observed in RF absence.

4.6. Quench flow experiments

4.6.1. Quench flow run

In quench flow the separately prepared RCs and RFs were mixed together and allowed to react for short length of time (usually 0.005 - 4 s, depending on reaction rate). In this way a series of time points was obtained and amounts of released and unreleased peptide for each time point were determined by scintillation counting. These series were fitted with exponential functions to determine rate constants. Both RC and RF mixes were prepared in PM with adjusted pH containing 0.1 mM of tyrosine and phenylalanine. The RC mix contained 0.2 µM of RCs and 120 units of Ribolock. The RF mix contained 4 µM of RF. Both mixes were loaded into the syringes connected to a quench flow instrument (RQF-3, KinTek). For each time point 20 µL of each reaction mix was loaded from the syringes into the instrument where they were pre-warmed to

37°C, automatically mixed, allowed to react for a set time at 37°C and quenched with formic acid (FA) to the final FA concentration of 17%. The acid was used to stop the reaction and to precipitate the RCs with unreleased peptide. At pH > 8 the RC syringe was cooled with ice to avoid spontaneous hydrolysis of the peptidyl-tRNA ester linkage that occurs at high pH. Aliquots were taken from the RC syringe before and after a time series to check for spontaneous hydrolysis. They were manually quenched with 50% FA to the final concentration of 17% and further treated as the rest of the samples. The quenched samples were collected to Eppendorf tubes with 25 µL 17% FA and cooled on ice.

4.6.2. Scintillation counting of quench flow samples

To separate the fractions of released and non-released peptide the samples were centrifuged for 15 min at 20817 x g at 4°C. The supernatants containing released peptide were removed and the pellets containing unreleased peptide were dissolved in 120 µL of 0.5 M KOH by incubating at 37°C for 10 min. The amount of radioactivity in pellet (P) and supernatant (S) was determined by counting in Quicksafe Flow 2 scintillation liquid in Beckman Coulter LS 6500 counter.

4.6.3. Treatment of quench flow data

A fraction of unreleased peptide was calculated as P/(P+S), plotted against reaction time and fitted with a double exponential function $y = A_{fast} \cdot e^{(-x / tfast)} + A_{slow} \cdot e^{(-x / tslow)} + y_0$. The rate constants (k) and their standard deviations (σ_k) were determined from corresponding release times (t) obtained from the fitting: $k = 1 / t$, $\sigma_k = \sigma_t / t^2$. The sum of amplitudes from both phases and its σ value were calculated as $A_{sum} = A_{fast} + A_{slow}$ and $\sigma_{Asum} = (\sigma_{Afast}^2 + \sigma_{Aslow}^2)^{1/2}$. Percent of an amplitude corresponding to the fast phase was calculated as $\%A_{fast} = A_{fast} / A_{sum} \cdot 100\%$. Its σ value was calculated as: $\sigma_{\%Afast} = \%A_{fast} \cdot [(\sigma_{\%Afast} / \%A_{fast})^2 + (\sigma_{Asum} / A_{sum})^2]^{1/2}$

4.7. Stopped flow experiments

4.7.1. Stopped flow run

In these experiments fluorescent RCs were rapidly mixed with release factors in a stopped flow instrument (SX-20, Applied Photophysics) and stopped in an observation cell. It was irradiated with monochromatic light and the change in fluorescence signal caused by peptide release was recorded as a function of time. The RC mix contained 0.2 µM of fluorescent RCs in PM buffer. The RF mix contained 4 µM (for mRF2) or 8 µM (for uRF1) of release factors in PM. Both mixes were centrifuged for 3 min at 20817 x g at 4°C to remove air bubbles and then loaded into

the syringes of the stopped flow instrument. The kinetics of peptide release was monitored at 37°C as a change in fluorescence signal after rapid mixing of equal volumes (usually 60 μL) of RC and RF mixes.

4.7.2. Treatment of stopped flow data

Each experiment generated 6-8 traces that were averaged to obtain an averaged trace. The rate constants and their σ values were obtained from fitting the time course with a triple exponential model: $y = A_1 \cdot e^{-k1 \cdot x} + A_2 \cdot e^{-k2 \cdot x} + A_3 \cdot e^{-k3 \cdot x} + c$ The additional rate constant k_1 not observed in quench flow experiments was around 100 s^{-1} and probably was the rate of binding of RF to the ribosome. It could not be measured in quench flow because of technical limitations: the shortest possible reaction time in quench flow was 0.005 s while in stopped flow it is ten times shorter: 0.0005 s. The percentage of A_{fast} and its standard deviation were calculated as for quench flow data.

4.8. Determining rates of release on UGG codon

The rate of release by unmethylated RF1 on a sense codon UGG was measured. The experiments were done either in a quench flow device or on a bench top. The rates obtained by these two methods did not differ. RC and RF mixes were prepared in PM with pH adjusted to 7.5 containing 0.1 mM tyrosine and phenylalanine. The RC mix contained 0.1 μM of RCs and 120 units of Ribolock. The RF mix contained 0.5 or 1 μM of RF. The concentration of free Mg^{2+} was reduced to 3 mM by adding 3 mM of GTP where indicated. Quench flow experiments were done as described in "Quench flow experiments". For bench-top experiments the mixes were shortly pre-incubated at 37°C and mixed together to start the reaction. Aliquots were taken at different time points and quenched with 50% FA to a final concentration of 17%. The quenched samples were processed and data treated as described in "Quench flow experiments", except that the time series at 2 mM Mg were fitted with a single exponential function.

4.9. Determining active concentration of release factors

Active concentration of RF1 and RF2 was determined by performing a series of reactions with constant RC concentration and increasing concentrations of RF. 50 μL RC mix containing 2.6 pmol RC in PM was mixed with 50 μL of RF mix containing 0 – 50 pmol RF in PM, allowed to react for 15 s and quenched with 50 μL of 50% FA to a final concentration of 17%. The samples were treated as described in "Quench flow experiments". The amount of released peptide in pmol was calculated by multiplying a total RC amount (2.6 pmol) by a fraction of released peptide.

The released peptide in pmol was plotted against RF concentration in pmol. The beginning of a plateau of the curve indicated when RCs and active RFs were at the same concentration. The active concentration was determined as a an active RF percentage of total RF at the plateau starting point. The active concentration of RF1 was 15%, or RF2 – 12%.

4.10. Other components of the in vitro translation system

Elongation factors EF-Tu, EF-Ts and EF-G, and Phe-tRNA synthetase were purified as described (Ehrenberg et al., 1990). Release factors were from Dr. Valerie Heurgue-Hamard (Institut de Biologie Physico-Chimique, France) and prepared as in (Dincbas-Renqvist et al., 2000).

5. Acknowledgements

I would like to thank Dr. Michael Pavlov for agreeing to be my supervisor, spending so much time helping me and teaching all the methods used in this project, for sharing some of his endless knowledge and for his kindness and patience.

I am grateful to the members of the group of Professor Måns Ehrenberg, especially Dr. Galyna Bartish, Anneli Borg and Kaweng Ieong for their help and advice and to Måns himself for encouraging to look deeper into the scientific meaning of my experiments.

6. References

Beringer, M., and Rodnina, M.V. (2007). The ribosomal peptidyl transferase. Mol Cell *26*, 311-321.

Bjornsson, A., Mottagui-Tabar, S., and Isaksson, L.A. (1996). Structure of the C-terminal end of the nascent peptide influences translation termination. Embo J *15*, 1696-1704.

Brunelle, J.L., Shaw, J.J., Youngman, E.M., and Green, R. (2008). Peptide release on the ribosome depends critically on the 2' OH of the peptidyl-tRNA substrate. Rna *14*, 1526-1531.

Dincbas-Renqvist, V., Engstrom, A., Mora, L., Heurgue-Hamard, V., Buckingham, R., and Ehrenberg, M. (2000). A post-translational modification in the GGQ motif of RF2 from Escherichia coli stimulates termination of translation. Embo J *19*, 6900-6907.

Ehrenberg, M., Rojas, A.M., Weiser, J., and Kurland, C.G. (1990). How many EF-Tu molecules participate in aminoacyl-tRNA binding and peptide bond formation in Escherichia coli translation? J Mol Biol *211*, 739-749.

Freistroffer, D.V., Kwiatkowski, M., Buckingham, R.H., and Ehrenberg, M. (2000). The accuracy of codon recognition by polypeptide release factors. Proc Natl Acad Sci U S A *97*, 2046-2051.

Frolova, L.Y., Tsivkovskii, R.Y., Sivolobova, G.F., Oparina, N.Y., Serpinsky, O.I., Blinov, V.M., Tatkov, S.I., and Kisselev, L.L. (1999). Mutations in the highly conserved GGQ motif of class 1 polypeptide release factors abolish ability of human eRF1 to trigger peptidyl-tRNA hydrolysis. Rna *5*, 1014-1020.

Green, R., and Lorsch, J.R. (2002). The path to perdition is paved with protons. Cell *110*, 665-668.

Heurgue-Hamard, V., Champ, S., Engstrom, A., Ehrenberg, M., and Buckingham, R.H. (2002). The hemK gene in Escherichia coli encodes the N(5)-glutamine methyltransferase that modifies peptide release factors. Embo J *21*, 769-778.

Ito, K., Uno, M., and Nakamura, Y. (2000). A tripeptide 'anticodon' deciphers stop codons in messenger RNA. Nature *403*, 680-684.

Jin, H., Kelley, A.C., Loakes, D., and Ramakrishnan, V. (2010). Structure of the 70S ribosome bound to release factor 2 and a substrate analog provides insights into catalysis of peptide release. Proc Natl Acad Sci U S A *107*, 8593-8598.

Johansson, M., Ieong, K.W., Trobro, S., Strazewski, P., Aqvist, J., Pavlov, M.Y., and Ehrenberg, M. (2011). pH-sensitivity of the ribosomal peptidyl transfer reaction dependent on the identity of the A-site aminoacyl-tRNA. Proc Natl Acad Sci U S A *108*, 79-84.

Johansson, M., Zhang, J., and Ehrenberg, M. (2012). Genetic code translation displays a linear trade-off between efficiency and accuracy of tRNA selection. Proc Natl Acad Sci U S A *109*, 131-136.
Katunin, V.I., Muth, G.W., Strobel, S.A., Wintermeyer, W., and Rodnina, M.V. (2002). Important contribution to catalysis of peptide bond formation by a single ionizing group within the ribosome. Mol Cell *10*, 339-346.
Kisselev, L., Ehrenberg, M., and Frolova, L. (2003). Termination of translation: interplay of mRNA, rRNAs and release factors? Embo J *22*, 175-182.
Klaholz, B.P. (2011). Molecular recognition and catalysis in translation termination complexes. Trends Biochem Sci *36*, 282-292.
Klaholz, B.P., Pape, T., Zavialov, A.V., Myasnikov, A.G., Orlova, E.V., Vestergaard, B., Ehrenberg, M., and van Heel, M. (2003). Structure of the Escherichia coli ribosomal termination complex with release factor 2. Nature *421*, 90-94.
Korostelev, A., Asahara, H., Lancaster, L., Laurberg, M., Hirschi, A., Zhu, J., Trakhanov, S., Scott, W.G., and Noller, H.F. (2008). Crystal structure of a translation termination complex formed with release factor RF2. Proc Natl Acad Sci U S A *105*, 19684-19689.
Korostelev, A.A. (2011). Structural aspects of translation termination on the ribosome. Rna *17*, 1409-1421.
Kuhlenkoetter, S., Wintermeyer, W., and Rodnina, M.V. (2011). Different substrate-dependent transition states in the active site of the ribosome. Nature *476*, 351-354.
Laurberg, M., Asahara, H., Korostelev, A., Zhu, J., Trakhanov, S., and Noller, H.F. (2008). Structural basis for translation termination on the 70S ribosome. Nature *454*, 852-857.
Loh, P.G., and Song, H. (2010). Structural and mechanistic insights into translation termination. Curr Opin Struct Biol *20*, 98-103.
Mora, L., Heurgue-Hamard, V., Champ, S., Ehrenberg, M., Kisselev, L.L., and Buckingham, R.H. (2003). The essential role of the invariant GGQ motif in the function and stability in vivo of bacterial release factors RF1 and RF2. Mol Microbiol *47*, 267-275.
Nakahigashi, K., Kubo, N., Narita, S., Shimaoka, T., Goto, S., Oshima, T., Mori, H., Maeda, M., Wada, C., and Inokuchi, H. (2002). HemK, a class of protein methyl transferase with similarity to DNA methyl transferases, methylates polypeptide chain release factors, and hemK knockout induces defects in translational termination. Proc Natl Acad Sci U S A *99*, 1473-1478.
Rodnina, M.V., and Wintermeyer, W. (1995). GTP consumption of elongation factor Tu during translation of heteropolymeric mRNAs. Proc Natl Acad Sci U S A *92*, 1945-1949.
Shaw, J.J., and Green, R. (2007). Two distinct components of release factor function uncovered by nucleophile partitioning analysis. Mol Cell *28*, 458-467.

Shin, D.H., Brandsen, J., Jancarik, J., Yokota, H., Kim, R., and Kim, S.H. (2004). Structural analyses of peptide release factor 1 from Thermotoga maritima reveal domain flexibility required for its interaction with the ribosome. J Mol Biol *341*, 227-239.
Song, H., Mugnier, P., Das, A.K., Webb, H.M., Evans, D.R., Tuite, M.F., Hemmings, B.A., and Barford, D. (2000). The crystal structure of human eukaryotic release factor eRF1--mechanism of stop codon recognition and peptidyl-tRNA hydrolysis. Cell *100*, 311-321.
Sund, J., Ander, M., and Aqvist, J. (2010). Principles of stop-codon reading on the ribosome. Nature *465*, 947-950.
Trobro, S., and Aqvist, J. (2007). A model for how ribosomal release factors induce peptidyl-tRNA cleavage in termination of protein synthesis. Mol Cell *27*, 758-766.
Trobro, S., and Aqvist, J. (2009). Mechanism of the translation termination reaction on the ribosome. Biochemistry *48*, 11296-11303.
Vestergaard, B., Sanyal, S., Roessle, M., Mora, L., Buckingham, R.H., Kastrup, J.S., Gajhede, M., Svergun, D.I., and Ehrenberg, M. (2005). The SAXS solution structure of RF1 differs from its crystal structure and is similar to its ribosome bound cryo-EM structure. Mol Cell *20*, 929-938.
Vestergaard, B., Van, L.B., Andersen, G.R., Nyborg, J., Buckingham, R.H., and Kjeldgaard, M. (2001). Bacterial polypeptide release factor RF2 is structurally distinct from eukaryotic eRF1. Mol Cell *8*, 1375-1382.
Youngman, E.M., McDonald, M.E., and Green, R. (2008). Peptide release on the ribosome: mechanism and implications for translational control. Annu Rev Microbiol *62*, 353-373.
Zavialov, A.V., Mora, L., Buckingham, R.H., and Ehrenberg, M. (2002). Release of peptide promoted by the GGQ motif of class 1 release factors regulates the GTPase activity of RF3. Mol Cell *10*, 789-798.

7. Appendix

Table A1. The pH dependence of release rates by methylated RF1 measured in stopped flow. The percentage of amplitude of the fast rate (A_{fast}) is also provided.

pH	$[OH^-]$ (μM)	k_{fast} (s^{-1})	k_{slow} (s^{-1})	A_{fast} (%)
6.20	0.02	2.14 ±0.10	0.66 ±0.19	84.44 ±9.05
6.90	0.08	10.31 ±0.42	2.43 ±0.20	67.61 ±4.17
7.10	0.13	15.99 ±0.58	2.65 ±0.20	71.11 ±2.87
7.60	0.40	37.17 ±1.25	2.22 ±0.17	79.99 ±6.51
7.90	0.79	48.78 ±3.38	1.63 ±0.14	72.85 ±18.47
8.20	1.58	55.93 ±3.92	1.66 ±0.17	74.10 ±17.10
8.50	3.16	62.01 ±7.18	1.15 ±0.15	71.94 ±37.35

Table A2. The pH dependence of release rates by methylated RF1 measured in quench flow. A_{dom} is a percentage of dominant amplitude.

pH	$[OH^-]$ (μM)	k_{dom} (s^{-1})	k_{small} (s^{-1})	A_{dom} (%)
6.2	0.02	2.08 ±0.21	22.56 ±6.49	29.75 ±6.94
6.5	0.03	2.76 ±0.43	19.31 ±8.04	39.56 ±9.52
6.8	0.06	2.32 ±0.44	12.56 ±1.54	61.56 ±8.75
7.1	0.13	12.30 ±0.82	1.65 ±0.36	76.38 ±11.97
7.5	0.32	17.97 ±0.77	2.25 ±0.32	85.58 ±5.08
7.7	0.50	26.10 ±1.74	3.87 ±0.83	85.56 ±8.50
7.9	0.79	29.26 ±3.77	4.42 ±1.82	79.09 ±16.79
8.2	1.58	41.02 ±3.97	3.57 ±1.96	82.54 ±13.41
8.5	3.16	48.17 ±4.27	3.41 ±0.88	83.43 ±3.66

Table A3. The pH dependence of release rates by unmethylated RF1 measured in stopped flow. The percentage of amplitude of the fast rate (A_{fast}) is also provided.

pH	[OH^-] (μM)	k_{fast} (s^{-1})	k_{slow} (s^{-1})	A_{fast} (%)
6.2	0.02	1.00 ±0.03	0.54 ±0.03	69.72 ±1.35
6.5	0.03	1.73 ±0.00	0.70 ±0.00	81.41 ±0.00
6.8	0.06	2.76 ±0.04	0.61 ±0.07	88.55 ±0.04
7.1	0.13	6.88 ±0.09	1.92 ±0.04	61.76 ±0.22
7.5	0.32	13.54 ±0.14	2.94 ±0.04	67.57 ±0.03
7.9	0.79	19.57 ±0.35	2.15 ±0.02	51.14 ±0.14
8.2	1.58	29.51 ±0.42	2.41 ±0.02	52.82 ±0.30
8.5	3.16	44.09 ±0.90	3.07 ±0.05	62.60 ±0.97

Table A4. The pH dependence of release rates by methylated RF2 measured in stopped flow. The percentage of amplitude of the fast rate (A_{fast}) is also provided.

pH	[OH^-] (μM)	k_{fast} (s^{-1})	k_{slow} (s^{-1})	A_{fast} (%)
6.2	0.02	3.08 ±0.02	0.94 ±0.05	86.99 ±1.88
6.5	0.03	5.14 ±0.04	1.17 ±0.06	88.40 ±1.18
6.8	0.06	8.02 ±0.05	1.40 ±0.04	86.87 ±0.89
7.1	0.13	18.06 ±0.30	3.76 ±0.06	64.94 ±1.80
7.5	0.32	27.76 ±0.38	2.85 ±0.04	73.07 ±2.87
7.9	0.79	34.91 ±0.36	2.21 ±0.03	77.50 ±2.50
8.2	1.58	36.55 ±0.44	1.88 ±0.04	78.13 ±2.90
8.5	3.16	25.61 ±0.27	1.18 ±0.02	74.29 ±1.77